

# Accuracy of maxillofacial prototypes fabricated by different 3-dimensional printing technologies using multi-slice and cone-beam computed tomography

Faezeh Yousefi<sup>1</sup>, Abbas Shokri<sup>2,\*</sup>, Maryam Farhadian<sup>3</sup>, Fariborz Vafaei<sup>4</sup>, Fereshte Forutan<sup>5</sup>

<sup>1</sup>Department of Oral and Maxillofacial Radiology, Hamadan University of Medical Sciences, Hamadan, Iran

<sup>2</sup>Dental Implant Research Center, Department of Oral and Maxillofacial Radiology, Hamadan University of Medical Sciences, Hamadan, Iran

<sup>3</sup>Department of Biostatistics, Dental Implants Research Center, School of Public Health and Research Center for Health Sciences, Hamadan University of Medical Sciences, Hamadan, Iran

<sup>4</sup>Department of Prosthodontics, Hamadan University of Medical Sciences, Hamadan, Iran

<sup>5</sup>General Dentist, Brilliant Clinic, Hamadan, Iran

## ABSTRACT

**Purpose:** This study aimed to compare the accuracy of 3-dimensional (3D) printed models derived from multidetector computed tomography (MDCT) and cone-beam computed tomography (CBCT) systems with different fields of view (FOVs).

**Materials and Methods:** Five human dry mandibles were used to assess the accuracy of reconstructions of anatomical landmarks, bone defects, and intra-socket dimensions by 3D printers. The measurements were made on dry mandibles using a digital caliper (gold standard). The mandibles then underwent MDCT imaging. In addition, CBCT images were obtained using Cranex 3D and NewTom 3G scanners with 2 different FOVs. The images were transferred to two 3D printers, and the digital light processing (DLP) and fused deposition modeling (FDM) techniques were used to fabricate the 3D models, respectively. The same measurements were also made on the fabricated prototypes. The values measured on the 3D models were compared with the actual values, and the differences were analyzed using the paired t-test.

**Results:** The landmarks measured on prototypes fabricated using the FDM and DLP techniques based on all 4 imaging systems showed differences from the gold standard. No significant differences were noted between the FDM and DLP techniques.

**Conclusion:** The 3D printers were reliable systems for maxillofacial reconstruction. In this study, scanners with smaller voxels had the highest precision, and the DLP printer showed higher accuracy in reconstructing the maxillofacial landmarks. It seemed that 3D reconstructions of the anterior region were overestimated, while the reconstructions of intra-socket dimensions and implant holes were slightly underestimated. (*Imaging Sci Dent 2021; 51: 41-7*)

**KEY WORDS:** Cone-Beam Computed Tomography; Printing, Three-Dimensional; Models, Anatomic; Multidetector Computed Tomography

## Introduction

Rapid prototyping (RP) is the process of 3-dimensional (3D) fabrication of physical objects using an actual model and computerized techniques. In the field of maxillofacial surgery and traumatology, RP can help in diagnosis and

simulation of osteotomy and resection techniques, implant placement, and treatment planning for facial defects.<sup>1,2</sup> In addition to clinical examinations, surgical models are often designed for preoperative assessments.<sup>3-5</sup>

Conventionally, multidetector computed tomography (MDCT) data are used to fabricate 3D models and to perform RP.<sup>6</sup> The use of novel imaging modalities such as cone-beam computed tomography (CBCT), with lower equipment costs, lower patient radiation dose, shorter scanning time, and higher image resolution<sup>7-9</sup> than traditional

Received July 3, 2020; Revised October 27, 2020; Accepted November 6, 2020

\*Correspondence to : Prof. Abbas Shokri

Department of Oral and Maxillofacial Radiology, Dental School, Hamadan University of Medical Sciences, Shahid Fahmideh St., Hamadan 654178-38741, Iran  
Tel) 98-912-286-1291, E-mail) dr.a.shokri@gmail.com

Copyright © 2021 by Korean Academy of Oral and Maxillofacial Radiology

This is an Open Access article distributed under the terms of the Creative Commons Attribution Non-Commercial License (<http://creativecommons.org/licenses/by-nc/3.0>) which permits unrestricted non-commercial use, distribution, and reproduction in any medium, provided the original work is properly cited.

Imaging Science in Dentistry · pISSN 2233-7822 eISSN 2233-7830

imaging techniques, is increasing as a way for presurgical treatment planning to benefit from 3D data.<sup>4,10</sup>

Primo et al.<sup>1</sup> found that 3D models reconstructed using a CBCT scanner with voxel sizes of 0.25 and 0.4 mm and an MDCT scanner using a pixel size of 0.3 mm showed acceptable dimensional errors and could be used for fabrication of prototypes in dentistry. Considering the different nature, geometry, and resolution of MDCT and CBCT,<sup>11,12</sup> it seems that the data obtained from these imaging modalities can be used to fabricate prototypes with variable dimensional accuracy.

The available RP technologies and the 3D printer types for this purpose are highly variable. Furthermore, 3D printers have a wide price range. A limited number of studies have compared the dimensional accuracy of prototypes fabricated by different types of 3D printers. Thus, this study aimed to compare the dimensional accuracy of the models fabricated by two 3D printers based on data obtained from MDCT and CBCT systems with different fields of view (FOVs).

## Materials and Methods

This experimental study was approved by the ethics committee of Hamadan University of Medical Sciences (IR. UMSHA.REC.1397.503). The sample size was calculated to be 5 dry human mandibles assuming a 90% study power, a 0.05 level of significance, a mean difference of 0.5, a standard deviation of 1, and a 0.95 correlation between the linear measurements of the same landmark using the 2 printers. To assess the ability and accuracy of reconstructing the anatomical landmarks, bone defects, and socket depth by the 3D printers, 5 dry human mandibles with no fractures, deformities, or severe erosion were selected.

In order to assess the accuracy of the bone defects reconstructed by the 3D printers, 2 defects measuring 3 × 3 mm were created at the site of the mandibular molars in the buccal and lingual cortical plates using a high-speed handpiece, and their superior-inferior and mesiodistal dimensions were measured using a digital caliper (Mitutoyo Corp., Kawasaki, Japan) to serve as the gold standard.

As anatomical landmarks, the length (superior-inferior dimension) and width (mesiodistal dimension) of the mental foramen and the distance between the alveolar crest and the inferior border of the mandible at the midline were also measured, as well as the central incisor dimensions, the mesiodistal width of the incisal region, and the occlusogingival distance between the mesioincisal line angle and the cemento-enamel junction.

In order to assess the accuracy of the intra-socket dimensions reconstructed by the 3D printers, the mesiodistal width of the mandibular first molar socket in the buccal area, the buccolingual width of the socket in the mesial area, and the depth of the socket at the mesiobuccal line angle were measured using a periodontal probe (Dental Williams color-coded Michigan probe) and recorded to serve as the gold standard.

Next, the mandibles underwent 64-slice MDCT (Philips Brilliance 64; Philips Medical Systems Nederland BV, Eindhoven, the Netherlands) imaging with the routine protocol for clinical applications (90 mA, 90 kVp, 480 μm pixel size). The CBCT images were obtained using a Cranex 3D CBCT scanner (Soredex, Tuusula, Finland) with exposure settings of 90 kVp, 6 mA, 6.12 s time, 6 × 8 cm<sup>2</sup> FOV, and 200 μm voxel size and a NewTom 3G CBCT scanner (Quantitative Radiology, Verona, Italy) with exposure settings of 110 kVp, variable amperage (mA), and 6-inch and 12-inch FOVs with voxel sizes of 200 μm and 400 μm, respectively. The images were stored in the Digital Imaging and Communications in Medicine (DICOM) format. The 3D models were fabricated through the process described below (Fig. 1).

The DICOM file was imported to the Simplant (Dentsply, Charlotte, NC, USA) image processing software (Fig. 1A). The samples were reconstructed based on Hounsfield units (Fig. 1B). Next, excess points were modified and eliminated, and the final file was prepared (Fig. 1B). The final file of the samples was exported in the STL format (Fig. 1C). Next, the STL file was imported to the 3D printer software (Mankati E180; Mankati, Shanghai, China) (Fig. 1D), and the printing settings including the speed, temperature, layer thickness, resolution, and density percentage were adjusted (Fig. 1D). Finally, the file was saved in G-Code format (Fig. 1E), the G-Code file was sent to the 3D printer, and the final prototype was manufactured (Fig. 2).

Two printers, which used the digital light processing (DLP; Planmeca Creo; Planmeca, Helsinki, Finland) and fused deposition modeling (FDM; Creator Pro; Flashforge, Zhejiang, China) techniques, respectively, were used to fabricate prototypes based on the imaging data of the mandibles. Using the FDM technique, thermoplastic material is extruded through a nozzle onto a build platform, while the DLP method uses a light-cured resin technique in which the resin is cured with a projector light source. The aim is to build a model upside down on the platform.<sup>13</sup>

The dimensions of the aforementioned anatomical landmarks and areas were measured on the 3D-printed models using a digital caliper, and the values were recorded. Thus, 5

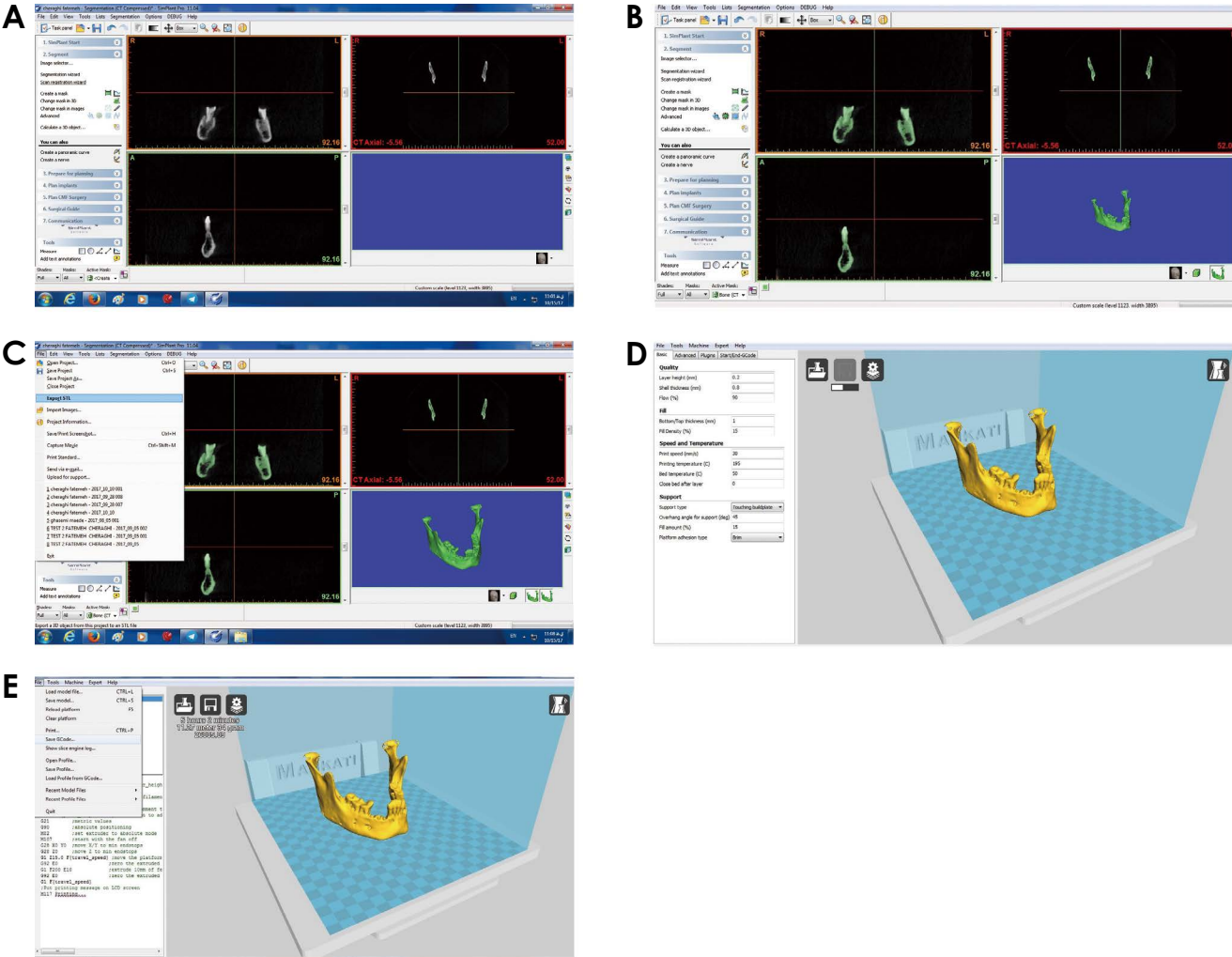


**Fig. 1.** A. DICOM file imported to Simplant (Dentsply, Charlotte, NC, USA) image processing software. B. Sample reconstruction is performed based on the Hounsfield units and modification and elimination of excess points. C. Preparing the final file of the sample in STL format. D. Importing the STL file to the 3D printer software and adjusting the printing settings, including the speed, temperature, layer thickness, resolution, and density percentage. E. Saving the file in G-Code format. DICOM: Digital Imaging and Communications in Medicine.

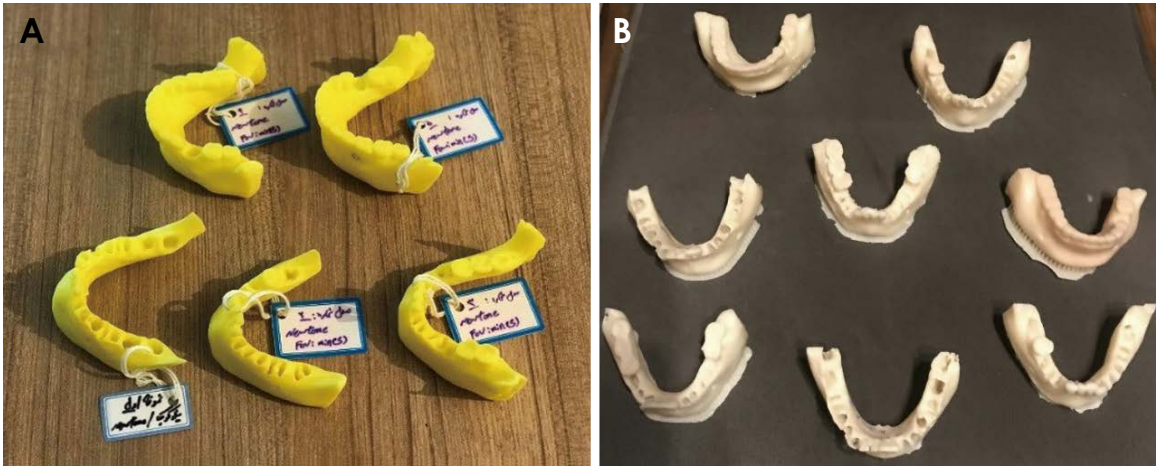


**Fig. 2.** A. Prototype samples made using the fused deposition modeling (FDM) technology. B. Prototype samples made using the digital light processing (DLP) technology.

dry mandibles were imaged by 4 different imaging systems, and 20 prototypes were fabricated using the DLP ( $n=20$ ) and FDM ( $n=20$ ) printing techniques. Two observers made the measurements twice at a 2-week interval. The values measured on the 3D models were compared with the actual values measured on the actual mandibles, and the differences were analyzed using the paired t-test. All statistical analyses were performed using SPSS version 21 (IBM Corp., Armonk, NY, USA) at a 0.05 level of significance.

## Results

In this study, in order to assess the intra- and inter-observer reliability, the intra-class correlation coefficient was calculated. The results showed inter- and intra-observer agreements  $>0.90$ . Table 1 compares the dimensions of the landmarks, bone defects, and sockets between the different imaging systems.

The measurements of both the FDM and DLP prototypes based on the data obtained from the Cranex 3D CBCT and NewTom small-FOV scanners had significant differences from the gold standard ( $P<0.05$ ). However, this difference was  $<0.7$  mm in all areas, which was clinically acceptable.<sup>14</sup> No significant difference was noted between the FDM and DLP printing techniques ( $P>0.05$ ), although the DLP printer showed smaller differences from the gold standard.

The measurements of the FDM and DLP prototypes derived from the NewTom large-FOV CBCT scanner had significant differences from the gold standard, which reached 2.20 mm in some areas. No significant difference was noted between the FDM and DLP printing techniques ( $P>0.05$ ). In MDCT, the differences for all areas were significant ( $P<0.05$ ), with larger measurements found in the anterior region and smaller measurements in intra-socket dimensions and implant holes. This difference reflects the larger pixel size of the CT scanner than the CBCT scanners. Both printers showed significant differences from the gold standard, reaching 2.80 mm in some areas. No significant difference was noted between the FDM and DLP printing techniques ( $P>0.05$ ).

## Discussion

The data required for RP and fabrication of 3D printing models are provided by different imaging modalities, such as MDCT and CBCT. The quality and accuracy of different types of RP systems have not been thoroughly investigated.

The CBCT scanners with small voxels had the highest

accuracy in reconstructing most of the landmarks. The CBCT scanner with large voxels and MDCT had a higher rate of errors in reconstructing the anatomical landmarks of the maxillofacial region. The magnitude of the errors was up to 0.7 mm for the small-voxel CBCT scanners and 2.2 mm for the large-voxel CBCT and MDCT scanners; this discrepancy reflects the difference in voxel sizes between the devices.

Regarding the reconstruction of the alveolar crest height from the inferior border of the mandible, the Cranex 3D showed the highest accuracy and MDCT showed the lowest accuracy. For this particular landmark, all 4 imaging modalities overestimated the values compared with the gold standard. Van Dessel et al. evaluated and compared 7 different CBCT scanners, including the ones evaluated in this study, and stated that all CBCT scanners could favorably reconstruct the mandible.<sup>11</sup>

For the reconstruction of socket dimensions, the Cranex 3D and NewTom CBCT scanners with small FOVs showed the highest accuracy, while the NewTom CBCT scanner with a large FOV and MDCT had the lowest accuracy. For this particular landmark, all 4 imaging systems underestimated the values compared with the gold standard.

In this study, the NewTom CBCT scanner with a large FOV and MDCT did not show acceptable accuracy in landmark measurements, and had considerable differences from the original model in all variables. Salemi et al. evaluated the accuracy of radiography when the FOV was changed, and concluded that a smaller FOV resulted in higher accuracy and quality of radiographs.<sup>15</sup>

Regarding the effects of the measurement accuracy of different imaging systems on the fabrication of prototypes, it may be stated that higher-resolution images would result in fabrication of a more accurate prototype, due to the higher accuracy of data imported to the printer. Shweel et al. evaluated the measurement accuracy of CBCT and MDCT scanners, and found that MDCT underestimated the depth by 1.7 mm on average and the width by 0.9 mm on average, while it overestimated the height by 1.7 mm on average. In contrast, the CBCT scanner underestimated the depth by 0.9 mm on average and the width by 0.7 mm on average, while it overestimated the height by 1 mm on average.<sup>16</sup> Considering the possibility of primary errors in imaging and the import process of data to the 3D printer, errors in the fabricated prototype are also expected.

In this study, prototypes fabricated from the NewTom large-FOV and MDCT scanners showed larger errors than the prototypes created using the Cranex 3D and NewTom small-FOV scanners, which was due to their higher spatial

**Table 1.** Comparison of the dimensions of different landmarks between digital light processing (DLP) and fused deposition modeling (FDM) printers based on the data derived from 4 imaging systems (mean  $\pm$  standard deviation, unit: mm)

Landmark	Gold standard	Imaging system	FDM	DLP
Right mental foramen, superior-inferior dimension	2.97 $\pm$ 0.62	Cranex	2.92 $\pm$ 0.63*	2.91 $\pm$ 0.63*
		NewTom s	2.84 $\pm$ 0.66*	2.80 $\pm$ 0.67*
		NewTom l	4.48 $\pm$ 1.28*	4.56 $\pm$ 1.26*
		MDCT	4.28 $\pm$ 1.03*	4.32 $\pm$ 1.01*
Left mental foramen, superior inferior dimension	2.63 $\pm$ 0.42	Cranex	2.50 $\pm$ 0.36*	2.56 $\pm$ 0.38*
		NewTom s	2.57 $\pm$ 0.47*	2.53 $\pm$ 0.44*
		NewTom l	4.30 $\pm$ 0.40*	4.36 $\pm$ 0.60*
		MDCT	4.22 $\pm$ 0.36*	4.27 $\pm$ 0.34*
Right mental foramen, mesiodistal dimension	4.01 $\pm$ 1.33	Cranex	3.90 $\pm$ 1.26*	3.93 $\pm$ 1.28*
		NewTom s	3.72 $\pm$ 1.36*	3.70 $\pm$ 1.38*
		NewTom l	6.28 $\pm$ 1.87*	6.21 $\pm$ 1.84*
		MDCT	6.49 $\pm$ 1.46*	6.42 $\pm$ 1.45*
Left mental foramen, mesiodistal dimension	3.29 $\pm$ 0.26	Cranex	3.17 $\pm$ 0.45	3.21 $\pm$ 0.43
		NewTom s	3.15 $\pm$ 0.60	3.20 $\pm$ 0.40
		NewTom l	5.32 $\pm$ 1.03*	5.41 $\pm$ 1.05*
		MDCT	6.11 $\pm$ 0.80*	6.04 $\pm$ 0.60*
Buccal bone defect, superior part	3.7 $\pm$ 0.89	Cranex	3.77 $\pm$ 0.94*	3.75 $\pm$ 0.95*
		NewTom s	3.83 $\pm$ 0.94*	3.78 $\pm$ 0.93*
		NewTom l	5.53 $\pm$ 1.12*	5.45 $\pm$ 1.14*
		MDCT	5.95 $\pm$ 1.34*	5.83 $\pm$ 1.33*
Buccal bone defect, mesial part	3.04 $\pm$ 0.6	Cranex	3.09 $\pm$ 0.62*	3.07 $\pm$ 0.62*
		NewTom s	3.15 $\pm$ 0.64*	3.11 $\pm$ 0.62*
		NewTom l	4.09 $\pm$ 0.92*	4.01 $\pm$ 0.89*
		MDCT	3.98 $\pm$ 0.61*	3.93 $\pm$ 0.63*
Lingual bone defect, superior part	3.28 $\pm$ 0.46	Cranex	3.38 $\pm$ 0.49*	3.35 $\pm$ 0.48*
		NewTom s	3.47 $\pm$ 0.47*	3.40 $\pm$ 0.46*
		NewTom l	5.20 $\pm$ 0.42*	5.16 $\pm$ 0.44*
		MDCT	5.34 $\pm$ 0.75*	5.26 $\pm$ 0.72*
Lingual bone defect, mesial part	2.99 $\pm$ 0.2	Cranex	3.02 $\pm$ 0.22*	3.00 $\pm$ 0.24*
		NewTom s	3.16 $\pm$ 0.15*	3.12 $\pm$ 0.17*
		NewTom l	4.08 $\pm$ 0.21*	4.02 $\pm$ 0.18*
		MDCT	3.93 $\pm$ 0.31*	3.88 $\pm$ 0.32*
Socket depth	9.37 $\pm$ 3.45	Cranex	9.16 $\pm$ 3.27*	9.1 $\pm$ 3.29*
		NewTom s	8.80 $\pm$ 3.12*	8.90 $\pm$ 3.22*
		NewTom l	7.25 $\pm$ 2.69*	7.36 $\pm$ 2.67*
		MDCT	6.95 $\pm$ 2.54*	7.08 $\pm$ 2.51*
Mesiodistal width of socket	8.41 $\pm$ 2.47	Cranex	8.25 $\pm$ 2.44*	8.27 $\pm$ 2.44*
		NewTom s	8.13 $\pm$ 2.28*	8.16 $\pm$ 2.27*
		NewTom l	7.40 $\pm$ 1.94*	7.51 $\pm$ 1.91*
		MDCT	7.56 $\pm$ 2.26*	7.49 $\pm$ 2.25*
Buccolingual width of socket	6.69 $\pm$ 0.8	Cranex	6.60 $\pm$ 0.76*	6.63 $\pm$ 0.75*
		NewTom s	6.49 $\pm$ 0.74*	6.57 $\pm$ 0.76*
		NewTom l	5.77 $\pm$ 0.63*	5.88 $\pm$ 0.61*
		MDCT	4.91 $\pm$ 0.63*	4.99 $\pm$ 0.62*

**Table 1.** Continued

Landmark	Gold standard	Imaging system	FDM	DLP
Distance between the alveolar crest and inferior border of mandible	30.57 ± 4.78	Cranex	30.69 ± 4.73*	30.68 ± 4.72*
		NewTom s	30.75 ± 4.74*	30.70 ± 4.76*
		NewTom l	31.36 ± 4.54*	31.34 ± 4.54*
		MDCT	32.07 ± 4.40*	32.01 ± 4.10*
Central incisor, mesiodistal	5.01 ± 0.18	Cranex	5.11 ± 0.09*	5.09 ± 0.13*
		NewTom s	5.10 ± 0.11*	5.07 ± 0.13*
		NewTom l	5.39 ± 0.19*	5.42 ± 0.20*
		MDCT	5.11 ± 0.16*	5.09 ± 0.15*
Central incisor, incisogingival	10.1 ± 2.89	Cranex	10.04 ± 2.87*	10.05 ± 2.88*
		NewTom s	9.94 ± 2.95*	9.96 ± 2.94*
		NewTom l	9.29 ± 2.88*	9.52 ± 2.89*
		MDCT	9.18 ± 2.67*	9.19 ± 2.67*

\*:  $P < 0.05$  compared with the gold standard by t-test

resolution. Spatial resolution is strongly influenced by pixel size. The pixel size is 200 µm in the Cranex 3D and NewTom small-FOV devices, while it is 400 µm in the NewTom large-FOV device and 480 µm in the MDCT scanner.

The printer type also affects the accuracy of prototype dimensions. The material used for the FDM technology is polylactic acid (PLA), while the Detax free print model resin is used for the DLP printer. Using the FDM technique for the fabrication of large objects can lead to dimensional changes in the prototype because the temperature varies in different layers. This temperature difference can lead to differences in the cooling speeds of the layers, which can generate internal stresses and lead to dimensional changes of the object. The DLP printer operates based on the layering technique, and each layer is set individually. Thus, less internal stress is generated as the result of final heating, resulting in smaller dimensional changes. PLA is the most commonly used material for the FDM technique, and the use of PLA in the FDM technology leads to more shrinkage in the actual dimensions than is observed for the resin that is the most commonly used material for DLP.<sup>17,18</sup>

Drummer et al. evaluated the factors affecting the dimensional accuracy of the models fabricated by the FDM technology using PLA along with tricalcium phosphate. They reported that the fabrication temperature and size of the samples influenced dimensional accuracy.<sup>19</sup> The general settings of the device (duration of the procedure, temperature, and diameter of layers) also have a significant effect on the results.

Each step in the process of RP is susceptible to errors, irrespective of the technique. Errors may occur during

several different steps, including data extraction from the scanner, image manipulation, the fabrication process, and finishing of the models. For instance, when processing images, some changes may occur due to the type of system used, the processing technique, or the scanning protocol. Dimensional errors must be minimized in order to avoid compromising the quality of models or their clinical application.<sup>1</sup>

The image acquisition technique in CT and CBCT also plays a fundamental role in this respect because image resolution is directly correlated with the 3D accuracy of the model surface. Errors that may occur in this phase are related to a number of factors, such as the layer thickness (main factor), tube angulation, voltage, patient movement, presence of metal objects in the oral cavity, and slice thickness in image reconstruction. Thinner slices yield more accurate models. A smaller voxel size also results in higher-quality and higher-resolution images, enabling the fabrication of a more accurate, higher-quality model.<sup>1</sup>

The resolution and contrast of each CBCT scanner depend on the detector type, size of FOV, voxel size, level of artifacts, number of basic images, and the algorithm used for image reconstruction.<sup>20,21</sup>

Although the DLP printer is more technologically advanced than the FDM printer and is more accurate, the difference between the 2 printers in the accuracy of landmark reconstruction was not significant in this study. However, the high cost of 3D printing was a major limitation encountered in this study. Future studies should investigate different types of 3D printers with different materials to assess their effect on the accuracy of radiographic image reconstruction.

In conclusion, 3D printers were reliable systems for maxillofacial reconstruction. In this study, scanners with smaller voxels had higher precision, and the DLP printer was more accurate than the FDM printer for reconstructing landmarks in the maxillofacial region. It seemed that the 3D reconstructions of the anterior region were overestimated, while the reconstructions of intra-socket dimensions and implant holes were slightly underestimated.

**Conflicts of Interest:** None

### Acknowledgements

This study was partially adapted from the MD thesis in Maxillofacial Radiology (thesis number: 9708224886), which was supported by the Vice-Chancellor of Research and Technology, Hamadan University of Medical Sciences, Hamadan, Iran.

### References

1. Primo BT, Presotto AC, de Oliveira HW, Gassen HT, Miguens SA Jr, Silva AN Jr, et al. Accuracy assessment of prototypes produced using multi-slice and cone-beam computed tomography. *Int J Oral Maxillofac Surg* 2012; 41: 1291-5.
2. Silva DN, Gerhardt de Oliveira M, Meurer E, Meurer MI, Lopes da Silva JV, Santa-Bárbara A. Dimensional error in selective laser sintering and 3D-printing of models for craniomaxillary anatomy reconstruction. *J Craniomaxillofac Surg* 2008; 36: 443-9.
3. Adolphs N, Liu W, Keeve E, Hoffmeister B. RapidSplint: virtual splint generation for orthognathic surgery - results of a pilot series. *Comput Aided Surg* 2014; 19: 20-8.
4. Metzger MC, Hohlweg-Majert B, Schwarz U, Teschner M, Hammer B, Schmelzeisen R. Manufacturing splints for orthognathic surgery using a three-dimensional printer. *Oral Surg Oral Med Oral Pathol Oral Radiol Endod* 2008; 105: e1-7.
5. Anssari Moin D, Derksen W, Verweij JP, van Merkesteyn R, Wismeijer D. A novel approach for computer-assisted template-guided autotransplantation of teeth with custom 3D designed/printed surgical tooling. An ex vivo proof of concept. *J Oral Maxillofac Surg* 2016; 74: 895-902.
6. Maschio F, Pandya M, Olszewski R. Experimental validation of plastic mandible models produced by a "low-cost" 3-dimensional fused deposition modeling printer. *Med Sci Monit* 2016; 22: 943-57.
7. Tsiklakis K, Syriopoulos K, Stamatakis HC. Radiographic examination of the temporomandibular joint using cone beam computed tomography. *Dentomaxillofac Radiol* 2004; 33: 196-201.
8. Hodez C, Griffaton-Taillandier C, Bensimon I. Cone-beam imaging: applications in ENT. *Eur Ann Otorhinolaryngol Head Neck Dis* 2011; 128: 65-78.
9. Miresmaeili A, Farhadian N, Mollabashi V, Yousefi F. Web-based evaluation of experts' opinions on impacted maxillary canines forced eruption using CBCT. *Dental Press J Orthod* 2015; 20: 90-9.
10. Zhang HR, Yin LF, Liu YL, Yan LY, Wang N, Liu G, et al. Fabrication and accuracy research on 3D printing dental model based on cone beam computed tomography digital modeling. *Hua Xi Kou Qiang Yi Xue Za Zhi* 2018; 36: 156-61.
11. Van Dessel J, Nicolielo LF, Huang Y, Coudyzer W, Salmon B, Lambrichts I, et al. Accuracy and reliability of different cone beam computed tomography (CBCT) devices for structural analysis of alveolar bone in comparison with multislice CT and micro-CT. *Eur J Oral Implantol* 2017; 10: 95-105.
12. Mischkowski RA, Pulsfort R, Ritter L, Neugebauer J, Brochhagen HG, Keeve E, et al. Geometric accuracy of a newly developed cone-beam device for maxillofacial imaging. *Oral Surg Oral Med Oral Pathol Oral Radiol Endod* 2007; 104: 551-9.
13. Metlerski M, Grocholewicz K, Jaroń A, Lipski M, Trybek G. Comparison of presurgical dental models manufactured with two different three-dimensional printing techniques. *J Healthc Eng* 2020; 2020: 8893338.
14. Kim SY, Shin YS, Jung HD, Hwang CJ, Baik HS, Cha JY. Precision and trueness of dental models manufactured with different 3-dimensional printing techniques. *Am J Orthod Dentofacial Orthop* 2018; 153: 144-53.
15. Salemi F, Shokri A, Maleki FH, Farhadian M, Dashti G, Ostovarad F, et al. Effect of field of view on detection of condyle bone defects using cone beam computed tomography. *J Craniofac Surg* 2016; 27: 644-8.
16. Shweel M, Amer MI, El-shamanhory AF. A comparative study of cone-beam CT and multidetector CT in the preoperative assessment of odontogenic cysts and tumors. *Egypt J Radiol Nucl Med* 2013; 44: 23-32.
17. Bastawrous S, Wake N, Levin D, Ripley B. Principles of three-dimensional printing and clinical applications within the abdomen and pelvis. *Abdom Radiol* 2018; 43: 2809-22.
18. Nestler N, Wesemann C, Spies BC, Beuer F, Bumann A. Dimensional accuracy of extrusion- and photopolymerization-based 3D printers: in vitro study comparing printed casts. *J Prosthet Dent* 2021; 125: 103-10.
19. Drummer D, Cifuentes-Cuellar S, Rietzel D. Suitability of PLA/TCP for fused deposition modeling. *Rapid Prototyp J* 2012; 18: 500-7.
20. Asaumi J, Kawai N, Honda Y, Shigehara H, Wakasa T, Kishi K. Comparison of three-dimensional computed tomography with rapid prototype models in the management of coronoid hyperplasia. *Dentomaxillofac Radiol* 2001; 30: 330-5.
21. Naitoh M, Nakahara K, Suenaga Y, Gotoh K, Kondo S, Arijji E. Comparison between cone-beam and multislice computed tomography depicting mandibular neurovascular canal structures. *Oral Surg Oral Med Oral Pathol Oral Radiol Endod* 2010; 109: e25-31.